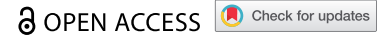


RESEARCH PAPER



## *Bifidobacterium longum* mediated tryptophan metabolism to improve atopic dermatitis via the gut-skin axis

Zhifeng Fang<sup>a,b</sup>, Tong Pan<sup>a,b</sup>, Lingzhi Li<sup>a,b</sup>, Hongchao Wang<sup>a,b</sup>, Jinlin Zhu<sup>a,b</sup>, Hao Zhang<sup>a,b,c,d</sup>, Jianxin Zhao<sup>a,b,d</sup>, Wei Chen<sup>a,b,c</sup>, and Wenwei Lu<sup>a,b,c,d,e</sup>

<sup>a</sup>State Key Laboratory of Food Science and Technology, Jiangnan University, Wuxi, Jiangsu, China; <sup>b</sup>School of Food Science and Technology, Jiangnan University, Wuxi, Jiangsu, China; <sup>c</sup>National Engineering Research Center for Functional Food, Jiangnan University, Wuxi, Jiangsu, China; <sup>d</sup>(Yangzhou) Institute of Food Biotechnology, Jiangnan University, Yangzhou, Jiangsu, China; <sup>e</sup>International Joint Research Laboratory for Pharmabiotics & Antibiotic Resistance, Jiangnan University, Wuxi, Jiangsu, China

### ABSTRACT

Gut microbial disturbance affects allergic diseases including asthma, atopic dermatitis (AD) via the aberrant immune response. Some *Bifidobacterium* species and strains have been reported to improve AD via modulating immune-microbe interactions in patients. However, the effective metabolites and mechanism of alleviating AD in bifidobacteria remain to be elucidated. This study aimed to explore the microbial metabolite and mechanism of *Bifidobacterium longum* to improve AD. Based on shotgun metagenomic sequencing and UHPLC Q-Exactive-MS targeted metabolic experiments *in vitro* and *in vivo*, we focused on tryptophan metabolism and indole derivatives, which are endogenous ligands for aryl hydrocarbon receptor (AHR). Indole-3-carbaldehyde (I3C), a tryptophan metabolite of *B. longum* CCFM1029 activated AHR-mediated immune signaling pathway to improve AD symptoms in animal and clinical experiments. *B. longum* CCFM1029 upregulated tryptophan metabolism and increased I3C to suppress aberrant T helper 2 type immune responses, but these benefits were eliminated by AHR antagonist CH223191. Furthermore, *B. longum* CCFM1029 reshaped gut microbial composition in AD patients, increased fecal and serum I3C, and maintained the abundance of *Lachnospiraceae* related to tryptophan metabolism of gut microbiota. The results suggested that based on the interactions of the gut-skin axis, *B. longum* CCFM1029 upregulated tryptophan metabolism and produced I3C to activate AHR-mediated immune response, alleviating AD symptoms. Indole derivatives, microbial metabolites of tryptophan, may be the potential metabolites of bifidobacteria to alleviate AD via the AHR signaling pathway.

### ARTICLE HISTORY

Received 22 December 2021  
Revised 14 February 2022  
Accepted 15 February 2022


### KEYWORDS


*Bifidobacterium longum*;  
tryptophan metabolism; gut-skin axis; aryl hydrocarbon receptors; indole-3-carbaldehyde; atopic dermatitis

## Introduction

Previous studies have demonstrated the differences in the bacterial diversity and composition of gut microbiota in patients with atopic dermatitis (AD) versus that in healthy controls.<sup>1,2</sup> Intestinal beneficial bacteria such as *Lactobacillus* and *Bifidobacterium* decrease but *Staphylococcus aureus*, *Clostridium difficile* increase in patients with AD.<sup>3–5</sup> Thus, gut microbiota is a potential target to alleviate AD because of the interactions of the gut-skin axis. Some probiotics have been demonstrated to alleviate AD via interacting with gut microbiota and immune responses in animal and clinical studies.<sup>6–8</sup> Although the effects of some specific probiotics have been revealed by numerous studies, the effective metabolites and mediating signaling pathway of probiotics to alleviate AD are far less elucidated.

Tryptophan is one of the essential amino acids and participates in gut immune regulation.<sup>9</sup> Metabolites from the direct metabolism of tryptophan by gut microbiota include indole and its derivatives, such as indole-3-acrylic acid (IA), indole acetic acid (IAA), indole-3-lactic acid (ILA), indole-3-propionic acid (IPA), and indole-3-carbaldehyde (I3C), and they are ligands for aryl hydrocarbon receptor (AHR).<sup>10</sup> AHR signaling plays an important role in immune modulation at barrier sites, such as skin and gut, through the interaction with various immune cells including dendritic cells and innate lymphoid cells.<sup>11</sup> Recent studies have demonstrated that catabolites from microbial tryptophan metabolism alleviate colitis and protect from *Candida albicans* infection via activating AHR to produce an anti-inflammatory cytokine IL-22 in

**CONTACT** Wenwei Lu  [luwenwei@jiangnan.edu.cn](mailto:luwenwei@jiangnan.edu.cn)  State Key Laboratory of Food Science and Technology, Jiangnan University, Wuxi, China

 Supplemental data for this article can be accessed on the [publisher's website](#).

© 2022 The Author(s). Published with license by Taylor & Francis Group, LLC.

This is an Open Access article distributed under the terms of the Creative Commons Attribution-NonCommercial License (<http://creativecommons.org/licenses/by-nc/4.0/>), which permits unrestricted non-commercial use, distribution, and reproduction in any medium, provided the original work is properly cited.

the intestine.<sup>12–14</sup> Serum I3C and IPA are negatively related to atherosclerosis and postoperative cardiac complication, and they have been considered as potential biomarkers for atherosclerotic disease.<sup>15</sup> Gut microbiota protect against radiation-induced damage through the increased *Lachnospiraceae*, *Enterococcaceae*, and their metabolites including propionate, I3C, and kynurenine (KYN) in mice.<sup>16</sup> These results suggest that indole derivatives are important for immune homeostasis and human health. In AD patients, tryptophan metabolism was reduced, and oral administration of I3C activated AHR binding to AHRE2 and AHRE4 in the promoter region of the thymic stromal lymphopoietin (*TSLP*) gene to suppress aberrant Th2-type immune responses.<sup>17,18</sup> This implies that microbial-derived tryptophan metabolites have the potential to alleviate the clinical symptoms of AD and trigger the interactions of the gut-skin axis.

The alleviating effects of *B. longum* strains on AD symptoms were demonstrated in our previous study.<sup>19</sup> They exerted the different effects on immunoregulation and gut microbial alterations in AD-like mice. However, the mechanism of action to attenuate AD remains to be elucidated. In this study, combined metagenomic sequencing analysis and targeted tryptophan metabolic analysis, the interactions between *B. longum* CCFM1029 and gut microbiota were revealed in animal and clinical dietary intervention experiments, and the mechanism of *B. longum* CCFM1029 to alleviate AD was elucidated. *B. longum* CCFM1029 reshaped gut microbial composition and upregulated tryptophan metabolism of gut microbiota to increase I3C, which mediated AHR signaling pathway to improve clinical symptoms in AD.

## Results

### *B. longum* CCFM1029 treatment upregulated tryptophan metabolism of gut microbiota in AD-like mice

An AD-like mouse model was induced using 2,4-dinitrofluorobenzene (DNFB) and the detailed methodology and progress referred to the part of animal model construction (materials and methods). To further explore the mechanism of *B. longum* strains to alleviate AD, an optimized

strain of bifidobacteria suppressing aberrant Th2 type responses was selected. Dead *B. longum* CCFM1029 did not alleviate AD-like symptoms in mice and suppress Th2-type immune responses (Figure S1). Dead *B. longum* CCFM1029 did not significantly reduce pathological score and ear thickness in AD-like mice. Furthermore, it could not significantly affect IgE, regulatory T cell (Treg) proportion, and IL-4 although it significantly increased the expression of IL-10 and IFN- $\gamma$ . It implied that the alleviating effects of *B. longum* CCFM1029 were associated with its metabolism and/or communication with gut microbiota. Therefore, we analyzed changes in gut microbiota in mice from the control, DNFB, and live CCFM1029 groups using shotgun metagenomic sequencing (n = 4–5). PCoA revealed the similarity or dissimilarity of gut microbial composition between groups (Figure 1a). Three groups were divided into different clusters by PC1 (23.93%) and PC2 (15.79%) influence factors and this showed the differences in gut microbiota in mice. Actinobacteria, Bacteroidetes, and Firmicutes were dominant bacteria in the three groups (Figure 1b). Actinobacteria (9.13%) was increased but Firmicutes (49.60%) was decreased in the DNFB group versus the control group (Actinobacteria and Firmicutes were 5.79% and 51.57%, respectively). Compared with the DNFB group, *B. longum* CCFM1029 treatment increased Actinobacteria (11.84%) and Firmicutes (50.13%) but reduced Bacteroidetes (32.13%). Proteobacteria had no significant alteration in the three groups, but Candidatus\_Saccharibacteria was significantly reduced in the DNFB group. At the genus level (relative abundance >0.5%), *Prevotella*, unclassified\_p\_Firmicutes, unclassified\_c\_Bacilli *Enterorhabdus*, *Alistipes*, *Streptococcus*, *Eggerthella*, *Enterococcus*, and *Adlercreutzia* were increased but unclassified\_f\_Lachnospiraceae, *Lactobacillus*, *Staphylococcus*, *Clostridium*, and unclassified\_p\_Candidatus\_Saccharibacteria were decreased in the DNFB group versus the control group (Figure 1c). Compared with the DNFB group, *B. longum* CCFM1029 treatment increased *Lactobacillus*, unclassified\_f\_Lachnospiraceae, unclassified\_p\_Candidatus\_Saccharibacteria, *Enterorhabdus*, *Clostridium*, and *Staphylococcus*



*B. longum* was only detected in the CCFM1029 group (Figure 2a). Furthermore, the relative abundances of *Enterorhabdus caecimuris* and *B. longum* were increased but other bacteria were reduced in the CCFM1029 group (Figure 2b). Based on the correlation analysis, fecal I3C was positively related to *B. longum* ( $p < .05$ ) (Figure 2c). However, the correlation was weak between I3C and *Enterorhabdus caecimuris*. Bacteria that contributed to tryptophan metabolism had complex interactions, for example, *Akkermansia muciniphila* was positively related to *Bacteroides thetaiotaomicron* ( $p < .05$ ) but it was negatively related to *B. longum*. To evaluate the ability of *B. longum* CCFM1029 to metabolize tryptophan, we determined indole derivatives using a resting cell culture system for *B. longum* CCFM1029 *in vitro*. *B. longum* CCFM1029 ( $8.5 \times 10^8$  CFU/mL) metabolized tryptophan to produce ILA ( $16967.43 \pm 1257.53$  ng/mL), IAA ( $3.89 \pm 1.78$  ng/mL), and I3C ( $11.20 \pm 0.64$  ng/mL), but IPA and IAA were not detected (Figure 2d, Figure S2). Additionally, we randomly selected some ineffective *B. longum* strains to analyze their abilities to produce I3C *in vitro* according to our previous

study results. Compared with *B. longum* CCFM1029, these strains produced lower I3C (Figure 2e). These results showed that *B. longum* CCFM1029 produced I3C via metabolizing tryptophan and had a potential to catabolize dietary tryptophan in the intestine.

### *B. longum* CCFM1029-induced I3C activated AHR to suppress Th2-type immune responses

AHR signaling contributes to the inhibition of the TSLP gene expression and suppresses aberrant Th2-type immune response in AD. Thus, we assumed that *B. longum* CCFM1029 alleviated AD symptoms via the AHR-mediated signaling pathway. CH223191, an antagonist for AHR, was used to block AHR. Hematoxylin-eosin staining showed inflammatory infiltration was increased on dorsal skin in the DNFB group versus the control group (Figure 3a). Compared with the DNFB group, *B. longum* CCFM1029, like the positive drug control I3C, significantly reduced dorsal swelling, but the alleviating effects of *B. longum* CCFM1029 were eliminated by CH223191 treatment. *B. longum* CCFM1029 and

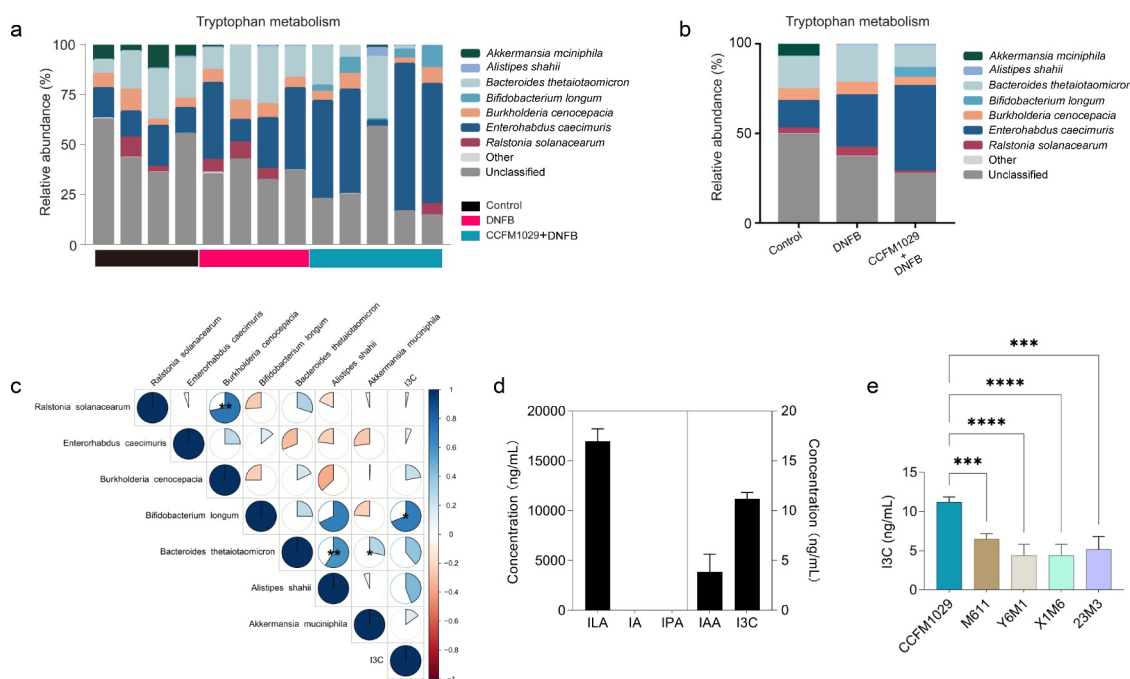


**Figure 2.** I3C was derived from *B. longum* CCFM1029 catabolizing tryptophan. (a-b) The analysis for the contribution of gut microbes for tryptophan metabolism. (c) The correlation analysis between gut microbial alteration and changes in I3C. (d) Evaluation of *B. longum* CCFM1029 metabolizing tryptophan *in vitro*. (e) Comparison for I3C production of *B. longum* strains metabolizing tryptophan *in vitro*. \*\*\* $p < .001$ , \*\*\*\* $p < .0001$  vs CCFM1029 group (one-way ANOVA test).

I3C treatments significantly reduced ear thickness and serum IgE compared with DNFB treatment (Figure 3b,c). To investigate the effects of AHR activation on *B. longum* CCFM1029-induced clinical manifestations, we assessed the expression of AHR. *B. longum* CCFM1029 and I3C treatments significantly increased AHR expression, but CH223191 treatment significantly blocked AHR activation (Figure 3d). Furthermore, the expression of TSLP and Th2-related cytokines were evaluated at the downstream pathway. *B. longum* CCFM1029 significantly decreased TSLP and thus suppressed the expressions of IL-4 and IL-5 through AHR activation compared with those in the DNFB group (Figure 3e-g). To explore whether AHR activation was related to I3C, we measured serum I3C, ILA, and IAA levels. I3C were significantly increased in the CCFM1029 group versus the DNFB group (Figure 3h), but serum ILA and IAA had no significant differences between the two groups (Figure S3). The results showed that *B. longum* CCFM1029 alleviated AD clinical symptoms by producing I3C to activate the AHR signaling pathway.

### *B. longum* CCFM1029 treatment increased I3C to alleviate AD symptoms in patients

The patients were collected and eligible subjects were randomized to the placebo (n = 43) and CCFM1029 groups (n = 44) (Figure 4a). There were no significant differences in baseline clinical characteristics between the placebo and CCFM1029 groups (Table 1). After 8 weeks of treatment, *B. longum* CCFM1029 significantly reduced scoring atopic dermatitis index (SCORAD) and the dermatology life quality index (DLQI) indicators versus before intervention, but placebo had no significant effects (Figure 4b). Furthermore, *B. longum* CCFM1029 treatment significantly reduced IgE versus before the intervention and after the placebo treatment, but it could not significantly reduce Th2-type cytokines (Figure 4c, Figure S4). Although *B. longum* CCFM1029 did not decrease IL-4 versus before the intervention, it reduced serum IL-4 compared with after placebo treatment ( $p = .078$ ). To analyze the effects of *B. longum* CCFM1029 on indole derivatives, changes in them were determined in fecal and serum samples.

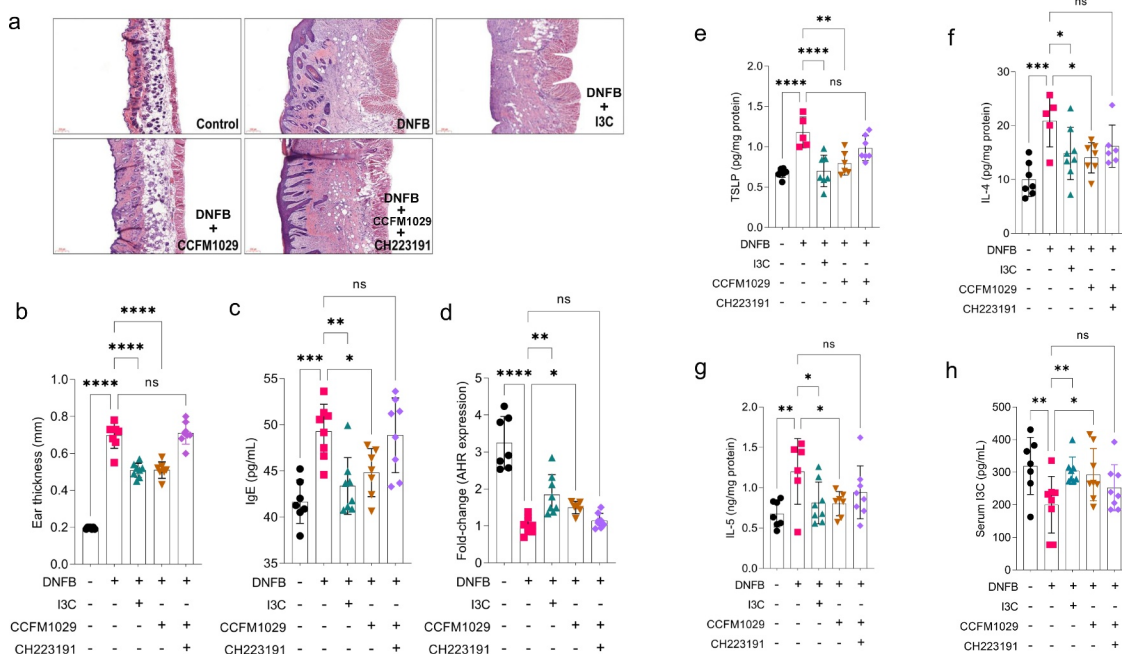


**Figure 3.** *B. longum* CCFM1029 inhibited AD symptoms via AHR-mediated immune responses. (a) Effects of *B. longum* CCFM1029 on skin inflammation. (b) Alteration of ear thickness in mice. (c) Changes in serum IgE ( $***p < .001$ ,  $****p < .0001$ , Two-way ANOVA followed Tukey's multiple comparisons test). (d) Fold-change for AHR expression. (e-g) TSLP, IL-4, and IL-5 in skin lesions. (h) Effects of *B. longum* CCFM1029 on serum I3C.  $*p < .05$ ,  $**p < .01$ ,  $***p < .001$ ,  $****p < .0001$  vs DNFB group (one-way ANOVA test). AHR, aryl hydrocarbon receptors; TSLP, thymic stromal lymphopoietin.

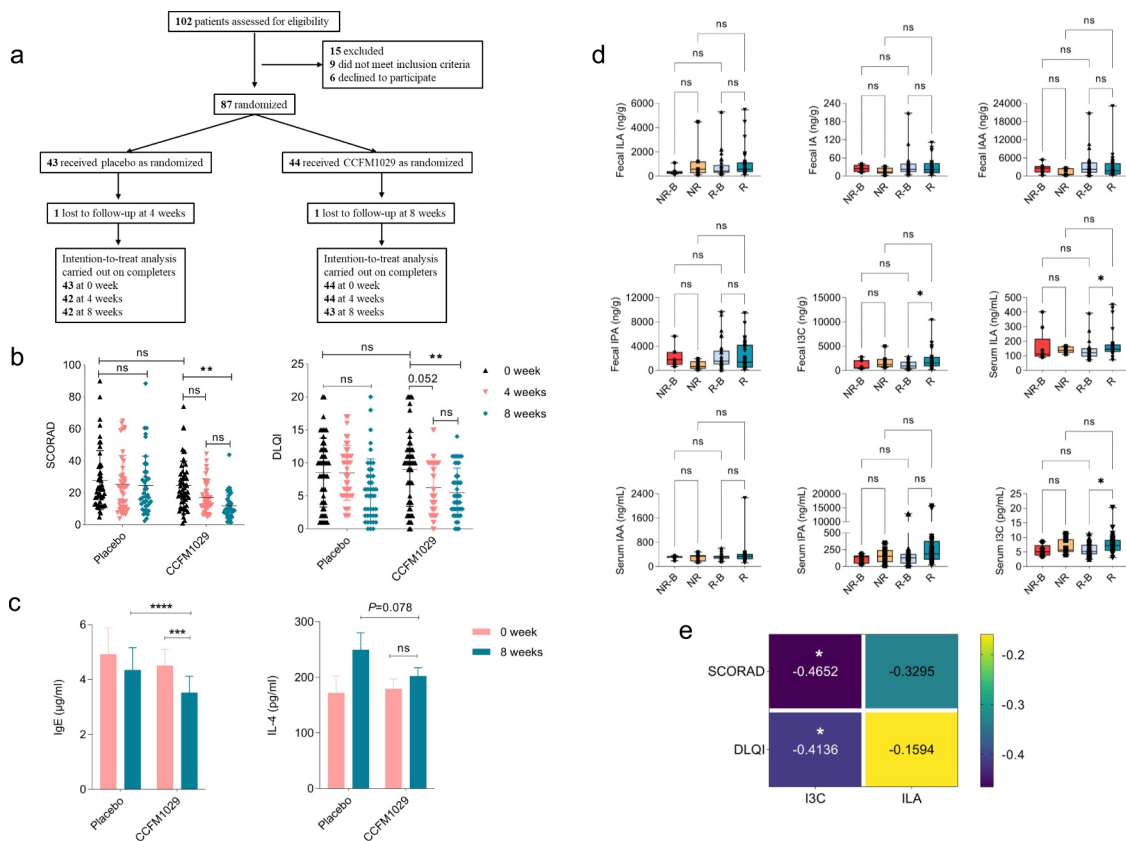


**Figure 4.** Effects of *B. longum* CCFM1029 on patients with AD. (a) Flowchart of the status of patients in the placebo and CCFM1029 groups. (b) Effect of *B. longum* CCFM1029 on SCORAD and DLQI indicators. (c) Effects of *B. longum* on serum markers. (d) Effects of *B. longum* CCFM1029 on indole derivatives in fecal and serum samples. \* $p < .05$  (Kruskal–Wallis test followed Dunn’s multiple comparisons test). SCORAD, scoring atopic dermatitis index; DLQI, dermatology life quality index; NR-B, non-response subgroup (before CCFM1029 treatment); NR, non-response subgroup (after CCFM1029 treatment); R-B, response subgroup (before CCFM1029 treatment); R, response subgroup (after CCFM1029 treatment).

**Table 1.** Baseline clinical characteristics of patients.

Characteristic	Placebo group (n = 43)	CCFM1029 group (n = 44)	<i>p</i> -value
Female sex, no. (%)	27 (62.79)	31 (70.45)	
Age, mean (SD), years	50.38 (10.80)	47.81 (13.73)	0.586
Height, mean (SD), cm	164.0 (5.88)	163.5 (4.10)	0.964
Weight, mean (SD), kg	59.5 (9.10)	60.09 (8.07)	0.552
SCORAD, mean (SD)	27.75 (19.32)	24.27 (14.85)	0.534
DLQI, mean (SD)	9.05 (5.19)	9.59 (5.63)	0.758
Use of corticosteroid drug, no. (%)	6 (13.95)	2 (4.55)	
Use of antibiotics, no. (%)	5 (11.63)	3 (6.82)	
History of hypersensitivity disease, no. (%)	8 (18.60)	6 (13.64)	

SCORAD, scoring atopic dermatitis index; DLQI, dermatology life quality index.

In the non-response subgroup (NR, no reduction in the SCORAD after CCFM1029 treatment,  $n = 12$ ), it had no significant effects on six indole derivatives both in fecal and serum samples versus before *B. longum* CCFM1029 intervention (NR-B, Figure 4d). In the response subgroup (R, a decrease in the SCORAD after CCFM1029

treatment,  $n = 31$ ), *B. longum* CCFM1029 significantly increased serum ILA, serum I3C, and fecal I3C compared with before the intervention (R-B). Furthermore, I3C was negatively related to SCORAD and DLQI ( $p < .05$ , Figure 4e) based on the correlation analysis, but ILA showed no significant negative correlation to them. Changes in I3C in patients were consistent with the results in the above animal experimental results. These results showed that *B. longum* CCFM1029 attenuated AD symptoms in patients via increasing I3C.

***B. longum* CCFM1029 treatment reshaped gut microbial composition and upregulated functional gene related to tryptophan metabolism of gut microbiota**

Placebo and *B. longum* CCFM1029 did not affect the Shannon index of gut microbiota (Figure S5). The NMDS analysis revealed that *B. longum*

CCFM1029, but not placebo, significantly altered beta diversity in patients ( $p < .004$ , Figure 5a, Figure S5). At the phylum level, placebo reduced the proportion of Actinobacteria and Proteobacteria and increased Firmicutes (Figure 5b). Compared with before *B. longum* CCFM1029 intervention (CCFM1029-B), the proportion of Bacteroidetes increased but Proteobacteria and Actinobacteria decreased in the NR subgroup (Figure 5c). However, the abundance of Proteobacteria was decreased, but Actinobacteria, Bacteroidetes, and Firmicutes were increased in the R subgroup. At the genus level (abundance  $>0.5\%$ ), LefSe analysis showed a higher abundance of *Phascolarctobacterium* and *Acidaminococcaceae* after placebo treatment (Figure 5d). Placebo treatment for 8 weeks reduced the proportions of Actinobacteria, Firmicutes, and *Proteobacteria* including *Acinetobacter*, *Bifidobacterium*, *Klebsiella*, *Haemophilus*, *Enterobacter*, *Weissella*, and *Collinsella* in patients. However, compared with CCFM1029-B and NR, *Lachnospiraceae* and *Sutterella* were the differential taxa in the R subgroup (Figure 5e). The relative abundance of *Sutterella* was significantly increased in the NR

subgroup but there was no significant effect on it in the R subgroup versus before *B. longum* CCFM1029 treatment. Furthermore, the proportion of *Lachnospiraceae* was significantly reduced in the NR subgroup but it was maintained in the R subgroup compared with the CCFM1029-B group (Figure 5f). Based on the PICRUSt gene functional analysis, *B. longum* CCFM1029 treatment significantly upregulated the abundance of functional genes related to tryptophan metabolism of gut microbiota (Figure 5g), and this was consistent with the increase in I3C in fecal and serum samples in patients with AD. The results showed that *B. longum* CCFM1029 treatment modulated gut microbiota and contributed to the increase in tryptophan metabolism of gut microbiota in patients with AD.

### Adverse events

There were no adverse events in patients during the intervention trial. Furthermore, *B. longum* CCFM1029 showed no significant effects on serum biochemical indices and urine indices in patients (Figure S6 and Table S3).

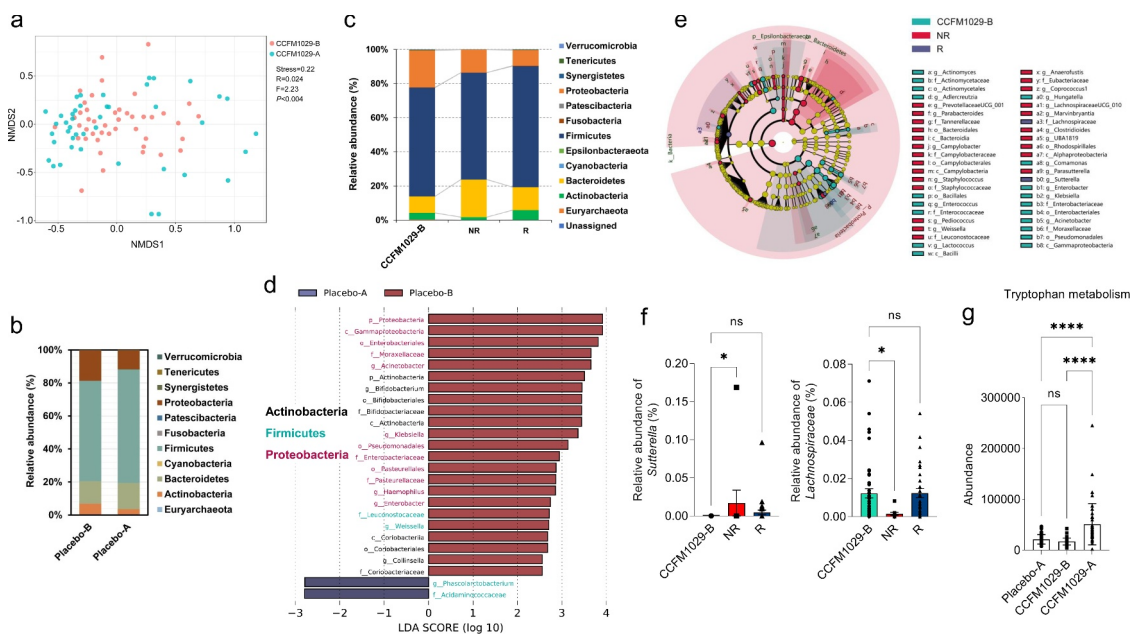


**Figure 5.** Effects of *B. longum* CCFM1029 on gut microbiota in patients. (a) NMDS analysis for  $\beta$  diversity of gut microbiota. (b-c) Gut microbial changes at the phylum level in patients. (d) LefSe analysis for differential taxa between before and after placebo intervention ( $p < .05$ , LDA score (log<sub>10</sub>) $>2.0$ ). (e) Cladogram for differentially abundant taxa in the CCFM1029-B group, NR subgroup, and R subgroup. (f) Changes in the proportions of *Sutterella* and *Lachnospiraceae*. (g) The abundance of functional genes related to tryptophan metabolism. \* $p < .05$  vs CCFM1029-B, \*\*\*\* $p < .0001$  (one-way ANOVA test). NMDS, non-metric multidimensional scaling. LefSe, linear discriminant analysis Effect Size.

## Discussion

This work explored the mechanism and effective metabolites of *B. longum* CCFM1029 to improve the clinical symptoms via experiments *in vitro* and *in vivo* and revealed the effects of *B. longum* CCFM1029 on immunoregulation via the gut-skin axis. In a clinical trial, the killed *Lactocaseibacillus rhamnosus* IDCC 3201 treatment for 12 weeks significantly decreased SCORAD in patients with moderate AD and showed great therapeutic potential for AD.<sup>20</sup> The results implied that dead probiotics might improve the clinical symptoms of diseases through the component from the cell wall. The dead *B. longum* CCFM1029, but not live *B. longum* CCFM1029, could not reduce the pathological score and inflammatory infiltration in the skin versus the DNFB group (Figure S1). The component of *B. longum* CCFM1029 itself could not suppress Th2-type response and ameliorate AD-like symptoms in mice. Therefore, these results suggested that the alleviation effect of *B. longum* CCFM1029 was associated with the metabolite from itself or the interactions with gut microbiota.

*B. longum* CCFM1029 upregulated the tryptophan metabolism in animal and clinical experiments (Figure 1d, Figure 5g). Tryptophan metabolism is a therapeutic target in diseases such as cancer and neurodegeneration through the kynurenine pathway, 5-hydroxytryptophan pathway, and microbial metabolism pathway.<sup>21,22</sup> Indole and indole derivatives are catabolites from microbial metabolism of tryptophan.<sup>11</sup> *B. longum* was only detected in the CCFM1029 group and positively associated with I3C production (Figure 2a–c). Although many bacteria contributed to the metabolism of tryptophan in the intestine, some species were unknown in fecal samples based on sequencing data. Additionally, based on HUMAnN2 analysis, nucleotide levels or protein levels of some annotated species were not mapped to pathways about tryptophan metabolism. Therefore, there were other and unclassified species contributing to tryptophan metabolism in Figure 2a, and their functions are to be elucidated in future studies. Additionally, compared with non-effective *B. longum* strains M611, Y6M1, X1M6, and 23 M3, *B. longum* CCFM1029 converted tryptophan into more I3C *in vitro* (Figure 2d,e). Consistent with

the results of the animal experiment and *in vitro*, *B. longum* CCFM1029 significantly improved AD symptoms via elevating fecal and serum I3C in patients (Figure 4d). Although the ILA was significantly elevated in the R subgroup compared with that in the R-B subgroup, I3C was much more sensitive to AHR than ILA.<sup>13</sup> Based on the correlation analysis, I3C, but not ILA, had a significant negative correlation to SCORAD and DLQI (Figure 4e), and thus I3C might be the effective metabolite to ameliorate AD. These results suggested that *B. longum* CCFM1029-produced I3C contributed to the improvement of AD symptoms.

Most indole derivatives such as ILA, IAA, and I3C, are the endogenous ligands for AHR, and AHR signaling-medicating immune responses contribute to treatment for AD.<sup>23,24</sup> The application of coal tar to improve AD depended on AHR activation to disturb Th2 signaling via dephosphorylation of STAT6.<sup>23</sup> AHR antagonist CH223191 eliminated the alleviation effects from *B. longum* CCFM1029 (Figure 3), which suggested *B. longum* CCFM1029-induced reduction of skin inflammation required AHR activation. This was consistent with the previous finding that AHR activation suppressed the expression of TSLP and thus reduced aberrant Th2 responses in mice with AD.<sup>18</sup> However, *B. longum* CCFM1029 significantly reduced serum IgE but had no significant effects on TSLP and Th2 responses in patients (Figure 3c). Oral administration of probiotics for 12 weeks showed no significant effects on blood markers such as IL-4, IL-5, and IL-13 in patients with AD,<sup>7</sup> which was consistent with our findings. Oral administration of heat-killed *L. plantarum* 0132-fermented juice for 8 weeks alleviated symptoms in patients with moderate AD and significantly reduced blood markers including IgE, specific IgE, and eosinophil cationic protein.<sup>25</sup> These controversial results suggested that the effects of probiotic strains on immune responses were specific.

Distant effects of gut microbiota have been verified in diseases such as asthma and depression. Alterations of gut microbial composition and function link to immune responses of skin diseases and this provides some insight into the development of AD. *B. longum* CCFM1029 altered gut microbial beta-diversity and modulated gut microbial composition (Figure 5a). In patients with AD, change in



beta-diversity but not alpha diversity was significant in a clinical trial,<sup>26</sup> which was consistent with our findings. *B. longum* CCFM1029 reduced the proportions of *Escherichia-Shigella* and *Klebsiella* that belonging to Proteobacteria. The high proportion of Proteobacteria might be associated with the development of AD. Higher *Escherichia-Shigella* and *Staphylococcus aureus* were harbored in allergic children in Estonia and Sweden.<sup>27</sup> Supplementation with bifidobacterial to pregnant women significantly reduced the risk of atopic dermatitis/eczema and had a lower proportion of Proteobacteria compared with the control group.<sup>28</sup> In the animal experiment, *B. longum* CCFM1029 significantly elevated the abundances of *Lactobacillus*, *Clostridium*, and unclassified\_f\_Lachnospiraceae (Figure 1c).  $\beta$ -glucan and *L. plantarum* LM1004 treatment decreased the expressions of Th2 and Th17 cell transcription factors through increasing *Lachnospiraceae*, *Bacteroides*, and *Roseburia* in mice with AD.<sup>29</sup> Increased *Lactobacillus* might contribute to the production of  $\gamma$ -aminobutyric acid (GABA), inhibiting skin itch.<sup>30</sup> In a cohort study on the natural course of AD in early childhood, a high proportion of *Streptococcus* and low *Clostridium* and *Akkermansia* were detected in children with persistent AD.<sup>31</sup>

*Phascolarctobacterium* was the differential bacteria in the placebo group (Figure 5d) and it was related to the development of Parkinson's disease and metabolic syndrome.<sup>32,33</sup> In the NR subgroup, *Sutterella* was increased but *Lachnospiraceae* was reduced versus the CCFM1029-B group. However, the abundances of both two bacteria showed no significant alteration in the R subgroup compared with the CCFM1029-B group. *Sutterella* is closely associated with the onset and development of gastrointestinal diseases and psychiatric disorders, such as inflammatory bowel disease, ulcerative colitis, and autism.<sup>34–37</sup> *Lachnospiraceae*, an SCFA-producing bacteria,<sup>38</sup> the delayed accumulation of SCFA was closely associated with the risk of development in allergen-sensitized AD infants in a longitudinal study.<sup>39</sup> Furthermore, *Lachnospiraceae*, with downstream metabolites such as propionate and I3C, protect against radiation in mice.<sup>16</sup> *B. longum* CCFM1029 treatment maintained the proportion of *Lachnospiraceae* in the R subgroup versus the CCFM1029-B group.

This suggested that gut microbiota might be involved in I3C production, but it was not enough to exert the alleviating effects on AD without *B. longum* CCFM1029 treatment. Therefore, *B. longum* CCFM1029 treatment reshaped gut microbial composition and contributed to the increase in tryptophan metabolism in patients with AD (Figure 5g). We did not exclude the contribution of gut microbiota *in situ* on tryptophan metabolism in the present study, which was a limitation. The effects of indol derivatives will be explored via a germ-free mouse model to assess the effects of gut microbiota on tryptophan metabolism in future studies.

In conclusion, the results showed that AD symptoms could be alleviated by affecting AHR agonist I3C produced by *B. longum* CCFM1029 triggering the communication between gut and skin. Additionally, indole derivatives, gut microbial metabolites of tryptophan, have the potential to affect immunoregulation in the host with a role of signal molecules and maybe a effective target to improve allergic diseases.

## Materials and methods

### Materials

IA, IAA, ILA, IPA, I3C, DNFB, AHR antagonist CH223191, methanol (gradient grade, Supelco), and acetonitrile (gradient grade, Supelco) were purchased from Sigma-Aldrich (St. Louis, MO, USA). Acetone and olive were purchased from Sinopharm Chemical Reagent Co., Ltd. (Shanghai, China).

### Bacterial preparation

*B. longum* strains (CCFM1029, M203F02M611 (M611), FSCDJY6M1 (Y6M1), FSHMX1M6 (X1M6), FXJWS23M3 (23 M3)) were stored at the Culture Collection of Food Microorganisms (Wuxi, Jiangsu, China). After consecutively activating for two generations, strains were cultured in MRS broth with 0.05% (w/v) L-cysteine-HCl (Sinopharm, Shanghai, China) under an anaerobic workstation (Electrotek AW400SG, Keighley, West Yorkshire, UK) at 37°C for 24–36 h. The detailed information that preparing bacterial cultures

referred to our previous article.<sup>19</sup> The number of viable bacteria was determined using the plate counting method.

### Animal model construction

Female C57BL/6 mice (SPF grade) aged 6 weeks were purchased from Charles River Laboratories (Beijing, China). Mice were fed under a facility with a controlled light cycle (12 h light/12 h dark), temperature (20–26°C), and humidity level (40–50%). Standard chow and water were available *ad libitum* during the experiment. After 1 week of adaption, AD-like symptoms were induced referring to our previous article.<sup>19</sup> Briefly, oral administration of *B. longum* CCFM1029 or sterile saline for 1 week, 2,4-dinitrofluorobenzene (DNFB, Sigma-Aldrich, St. Louis, MO, USA) was mixed with a substrate solution (acetone:olive oil = 4:1, v/v, Sinopharm, Shanghai, China) to make the sensitizing solution (0.5% and 0.2%). On day 15, 0.5% DNFB solution was painted on the shaved dorsal skin and left ear in mice. Then, 0.2% DNFB solution was painted in the same places to induce AD-like symptoms on days 19, 22, 25, and 28. The experimental flow chart was shown in Figure 6.

### Experiment supplementing I3C in mice with AD

Female mice were randomly divided into the control group, DNFB group, I3C group, CCFM1029 group, and AHR antagonist CH223191 (Sigma-Aldrich) group (n = 8). One week before model establishment, the mice were gavaged *B. longum* CCFM1029 suspension (diluting to 10<sup>9</sup> CFU/0.2 mL with sterile saline) once a day in the CH223191 and CCFM1029 groups until the end of the experiment, and 10 μM CH223191 (20 μL) was painted on the ear and skin for 30 min before *B. longum* CCFM1029 treatment.<sup>18</sup> The mice were gavaged 0.2 mL sterile saline in the control and DNFB groups, and oral administration of 0.2 mL I3C solution (10 μg/mL, Sigma-Aldrich) in the I3C group.

### Shotgun metagenomic sequencing for fecal samples of mice

Shotgun metagenomic sequencing of fecal samples (n = 4–5) was performed by Majorbio Biopharm Technology Co., Ltd. (Shanghai, China). The detailed information was referred to in a previous article.<sup>40</sup> Briefly, a library with an average insert size

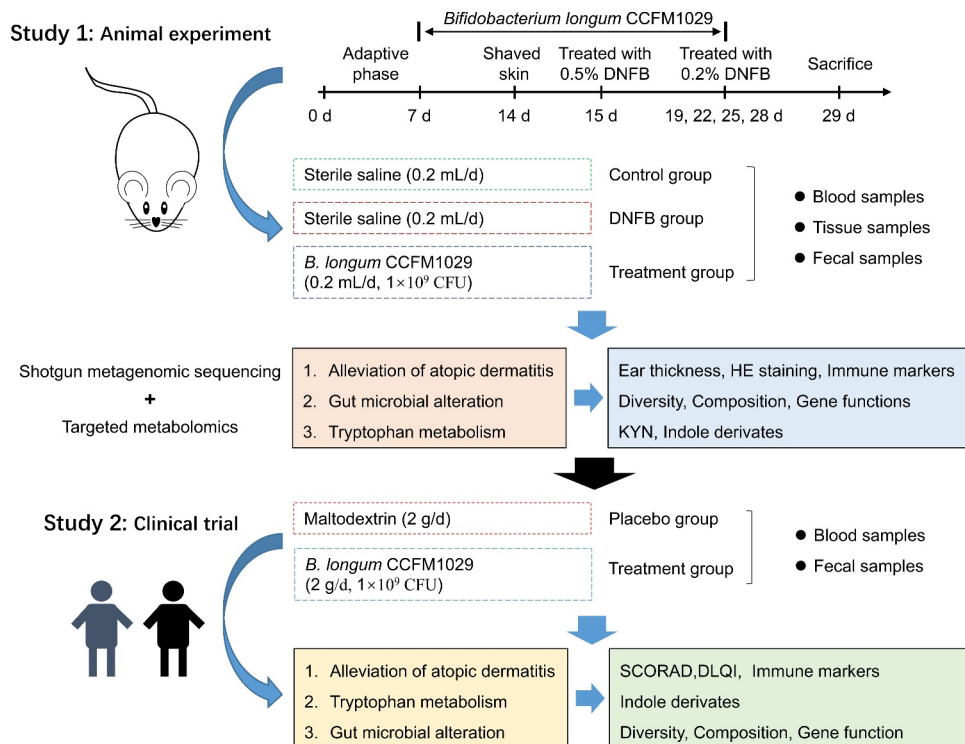


**Figure 6.** Experimental flow chart. HE: hematoxylin-eosin; KYN: Kynurenine.

of 400 bp was constructed for every sample and was sequenced using the Illumine NovaSeq platform (Illumine, San Diego, CA, USA). High-quality sequences were obtained after filtering raw data and quality control. The clean reads were assembled to generate contig using MEGAHIT (Table S1). Non-redundant gene sequences were aligned to the NCBI NR database and KEGG database using BLASTP (version 2.2.28+) to obtain detailed information for taxa and gene functions. Principal coordinates analysis (PCoA) was performed based on Jaccard distance. LEfSe was used to determine the differences in gene functions between the DNFB and CCFM1029 groups. The data were carried out on the Majorbio Cloud Platform (<http://www.majorbio.com>). The contribution of gut microbiota for tryptophan metabolism was performed using HuMAN2 (version 0.11.2).<sup>41</sup>

### **Recruitment of AD patients and sample collection**

The clinical evaluation was a randomized placebo-controlled trial. AD patients were recruited at the Tinghu People's hospital (Yancheng, Jiangsu, China) and AD clinical symptoms were diagnosed by dermatologists according to Hanifin & Rajka criteria. All patients provided written informed consents. Participants were ineligible if they had taken systemic corticosteroids and cyclosporine, or antibiotic and probiotic products in the previous 2 weeks, or signs of bacterial infection. All subjects (n = 102) were randomly divided into the placebo and CCFM1029 groups and the clinical baseline characteristics of patients were collected. Patients received daily a bag containing *B. longum* CCFM1029 lyophilized powder (10<sup>9</sup> CFU/2 g) or maltodextrin powder (2 g) for 8 weeks. Serum and fecal samples were collected and frozen at -80°C until for use.

### **16S rRNA amplicon sequencing**

In the clinical evaluation experiment, the total DNA of fecal samples was obtained using the FastDNA spin kit for feces (MP Biomedicals, Santa Ana, CA, USA). The V3-V4 region was amplified (341 F and 806 R) and sequenced using the Illumina sequencing platform (Miseq, Illumina Co., Santiago Canyon,

CA, USA). The 16S rRNA data were analyzed using the QIIME2 pipeline (open-source, <http://qiime2.org>). Non-metric multidimensional (NMDS) analysis was performed to reveal the differences between groups based on Bray-Curtis distance. The functional genes of microbiota were evaluated using the phylogenetic investigation of communities by reconstruction of unobserved states (PICRUSt).<sup>42</sup>

### **Determination of indole derivatives in serum and fecal samples**

Serum and fecal samples pretreatment, and the standard solution preparation were referred to supplementary material. The determination of indole derivatives was performed on a Vanquish UHPLC Q-Exactive Plus MS (Thermo Fisher, CA, USA) equipped with an ACQUITY UPLC BEH C18 column (Waters, Milford, Massachusetts; 1.7 μm, 2.1 × 100 mm). A binary solvent system composed of mobile phase A (acetonitrile, ACN, Supelco, Sigma-Aldrich) and mobile phase B (0.1% formic acid, Supelco, Sigma-Aldrich). The binary gradients were as follows: 5% A for 3 min, 5% A to 30% A for 6 min, 30% A to 100% A for 6 min, 100% A for 1.5 min, and re-equilibrated column with 5% A for 3.5 min. The total time was 20 min at a flow rate of 300 μl/min, and the column temperature was 35°C. The injection volume was 2 μL. Mass spectrometry was carried on a Q-Exactive Plus MS operating in positive ion mode. The conditions of heated electrospray ionization were as follows: ion spray voltage, 3.5 kV; capillary temperature, 320°C, heater temperature, 320°C, auxiliary gas volume flow, 15 arb, and sheath gas flow rate, 35 arb. The scan mode was a full-scan acquisition from 80 to 1200 m/z with a resolution of 70,000 and AGC target 3e6.

### **Indole derivatives determination from tryptophan metabolism of *B. longum* in vitro**

At the initial stationary phase of *B. longum* strain growth, the bacterial solution was centrifuged at 3400 × g at 4°C for 20 min. Removing the supernatant and bacteria were washed using phosphate-buffered saline (pH = 7.4). After re-centrifuge with the same condition, 1 mL M9 culture media (Table S2) was added to the tube and the bacteria were cultured for 48 h under anaerobic conditions.<sup>43</sup>

Then bacteria were centrifuged at 7000 × g under 4°C for 10 min to obtain supernatant. A 100 µL supernatant was mixed with 800 µL precooled methanol and the mixture was put on ice for 30 min to remove protein. The mixture was centrifuged at 15000 × g under 4°C for 10 min to obtain supernatant. After vacuum concentration and centrifuge treatment, the final sample was obtained for UHPLC Q-Exactive-MS analysis.

### Statistical analysis

The SPSS software (version 20.0, Chicago, Illinois, USA) and Origin Pro 9 software (Origin Lab Corporation, Wellesley Hills, Massachusetts, USA) were used to perform statistical analysis. A *p*-value <0.05 was indicated statistically significant.

### Acknowledgments

Thanks for the help of the Collaborative Innovation Center of Food Safety and Quality Control in Jiangsu Province.

### Disclosure statement

No potential conflict of interest was reported by the author(s).

### Ethics approval

The animal experiment was approved by the Ethical Committees of Jiangnan University (JN.No20191115c0480105[314] and JN.No20180115c2600531[5]). The clinical trial was approved by the Ethical Committees of Tinghu people's hospital (ethical approval No. ET2019030, Clinical Trial registry No. ChiCTR1900024199).

### Data availability statement

Shotgun sequencing data are available from the corresponding author, WWL, upon reasonable request. Due to participants of this study did not agree for their data to be shared publicly, 16S rRNA amplicon sequencing data in the clinical trial is not available.

### Funding

This work is supported by the National Natural Science Foundation of China (No. 31820103010, 32021005), 111project (Project 111, BP0719028), and the Postdoctoral Research Funding Scheme of Jiangsu Province (No. 2021K018A).

## References

- Marrs T, Jo JH, Perkin MR, Rivett DW, Witney AA, Bruce KD, Logan K, Craven J, Radulovic S, Versteeg SA, et al. Gut microbiota development during infancy: impact of introducing allergenic foods. *J Allergy Clin Immunol*. 2021;147(2):613–621.e9. doi:10.1016/j.jaci.2020.09.042.
- Lee MJ, Kang MJ, Lee SY, Lee E, Kim K, Won S, Suh DI, Kim KW, Sheen YH, Ahn K, et al. Perturbations of gut microbiome genes in infants with atopic dermatitis according to feeding type. *J Allergy Clin Immunol*. 2018;141(4):1310–1319. doi:10.1016/j.jaci.2017.11.045.
- Wang M, Karlsson C, Olsson C, Adlerberth I, Wold AE, Strachan DP, Martricardi PM, Aberg N, Perkin MR, Tripodi S, et al. Reduced diversity in the early fecal microbiota of infants with atopic eczema. *J Allergy Clin Immunol*. 2008;121(1):129–134. doi:10.1016/j.jaci.2007.09.011.
- Björkstén B, Sepp E, Julge K, Voor T, Mikelsaar M. Allergy development and the intestinal microflora during the first year of life. *J Allergy Clin Immunol*. 2001;108(4):516–520. doi:10.1067/mai.2001.118130.
- Watanabe S, Narisawa Y, Arase S, Okamatsu H, Ikenaga T, Tajiri Y, Kumemura M. Differences in fecal microflora between patients with atopic dermatitis and healthy control subjects. *J Allergy Clin Immunol*. 2003;111(3):587–591. doi:10.1067/mai.2003.105.
- Viljanen M, Savilahti E, Haahtela T, Juntunen-Backman K, Korpela R, Poussa T, Tuure T, Kuitunen M. Probiotics in the treatment of atopic eczema/dermatitis syndrome in infants: a double-blind placebo-controlled trial. *Allergy*. 2005;60(4):494–500. doi:10.1111/j.1398-9995.2004.00514.x.
- Navarro-López V, Ramírez-Boscá A, Ramón-Vidal D, Ruzafa-Costas B, Genovés-Martínez S, Chenoll-Cuadros E, Carrión-Gutiérrez M, Horga de la Parte J, Prieto-Merino D, Codoñer-Cortés FM. Effect of oral administration of a mixture of probiotic strains on scorad index and use of topical steroids in young patients with moderate atopic dermatitis: a randomized clinical trial. *JAMA Dermatol*. 2018;154(1):37–43. doi:10.1001/jamadermatol.2017.3647.
- Kwon MS, Lim SK, Jang JY, Lee J, Park HK, Kim N, Yun M, Shin MY, Jo HE, Oh YJ, et al. *Lactobacillus sakei* WIKIM30 ameliorates atopic dermatitis-like skin lesions by inducing regulatory t cells and altering gut microbiota structure in mice. *Front Immunol*. 2018;9:1905. doi:10.3389/fimmu.2018.01905.
- Gao J, Xu K, Liu H, Liu G, Bai M, Peng C, Li T, Yin Y. Impact of the gut microbiota on intestinal immunity mediated by tryptophan metabolism. *Front Cell Infect Microbiol*. 2018;8:13. doi:10.3389/fcimb.2018.00013.
- Sun M, Ma N, He T, Johnston LJ, Ma X. Tryptophan (Trp) modulates gut homeostasis via aryl hydrocarbon receptor (AhR). *Crit Rev Food Sci Nutr*. 2020;60(10):1760–1768. doi:10.1080/10408398.2019.1598334.

11. Agus A, Planchais J, Sokol H. Gut microbiota regulation of tryptophan metabolism in health and disease. *Cell Host Microbe*. 2018;23(6):716–724. doi:10.1016/j.chom.2018.05.003.
12. Lamas B, Richard ML, Leducq V, Pham HP, Michel ML, Da Costa G, Bridonneau C, Jegou S, Hoffmann TW, Natividad JM, et al. CARD9 impacts colitis by altering gut microbiota metabolism of tryptophan into aryl hydrocarbon receptor ligands. *Nat Med*. 2016;22(6):598–605. doi:10.1038/nm.4102.
13. Zelante T, Iannitti RG, Cunha C, De Luca A, Giovannini G, Pieraccini G, Zecchi R, D'Angelo C, Massi-Benedetti C, Fallarino F, et al. Tryptophan catabolites from microbiota engage aryl hydrocarbon receptor and balance mucosal reactivity via interleukin-22. *Immunity*. 2013;39(2):372–385. doi:10.1016/j.immuni.2013.08.003.
14. Borghi M, Pariano M, Solito V, Puccetti M, Bellet MM, Stincardini C, Renga G, Vacca C, Sellitto F, Mosci P, et al. Targeting the aryl hydrocarbon receptor with indole-3-aldehyde protects from vulvovaginal candidiasis via the IL-22-IL-18 cross-talk. *Front Immunol*. 2019;10:2364. doi:10.3389/fimmu.2019.02364.
15. Cason CA, Dolan KT, Sharma G, Tao M, Kulkarni R, Helenowski IB, Doane BM, Avram MJ, McDermott MM, Chang EB, et al. Plasma microbiome-modulated indole- and phenyl-derived metabolites associate with advanced atherosclerosis and postoperative outcomes. *J Vasc Surg*. 2018;68(5):1552–1562.e7. doi:10.1016/j.jvs.2017.09.029.
16. Guo H, Chou WC, Lai Y, Liang K, Tam JW, Brickey WJ, Chen L, Montgomery ND, Li X, Bohannon LM, et al. Multi-omics analyses of radiation survivors identify radioprotective microbes and metabolites. *Science*. 2020;370. doi:10.1126/science.aay9097.
17. Chng KR, Tay AS, Li C, Ng AH, Wang J, Suri BK, Matta SA, McGovern N, Janela B, Wong XF, et al. Whole metagenome profiling reveals skin microbiome-dependent susceptibility to atopic dermatitis flare. *Nat Microbiol*. 2016;1(9):16106. doi:10.1038/nmicrobiol.2016.106.
18. Yu J, Luo Y, Zhu Z, Zhou Y, Sun L, Gao J, Sun J, Wang G, Yao X, Li W. A tryptophan metabolite of the skin microbiota attenuates inflammation in patients with atopic dermatitis through the aryl hydrocarbon receptor. *J Allergy Clin Immunol*. 2019;143(6):2108–2119.e12. doi:10.1016/j.jaci.2018.11.036.
19. Fang Z, Li L, Liu X, Lu W, Zhao J, Zhang H, Chen W. Strain-specific ameliorating effect of *Bifidobacterium longum* on atopic dermatitis in mice. *J Funct Foods*. 2019;60:103426. doi:10.1016/j.jff.2019.103426.
20. Jeong K, Kim M, Jeon SA, Kim YH, Lee S. A randomized trial of *Lactobacillus rhamnosus* IDCC 3201 tyndallizate (RHT3201) for treating atopic dermatitis. *Pediatr Allergy Immunol*. 2020;31:783–792. doi:10.1111/pai.13269.
21. Platten M, Nollen EAA, Röhrig UF, Fallarino F, Opitz CA. Tryptophan metabolism as a common therapeutic target in cancer, neurodegeneration and beyond. *Nat Rev Drug Discov*. 2019;18(5):379–401. doi:10.1038/s41573-019-0016-5.
22. Rothhammer V, Borucki DM, Tjon EC, Takenaka MC, Chao CC, Ardura-Fabregat A, de Lima KA, Gutiérrez-Vázquez C, Hewson P, Staszewski O, et al. Microglial control of astrocytes in response to microbial metabolites. *Nature*. 2018;557(7707):724–728. doi:10.1038/s41586-018-0119-x.
23. van den Bogaard EH, Bergboer JG, Vonk-Bergers M, van Vlijmen-willems IM, Hato SV, van der Valk PG, Schröder JM, Joosten I, Zeeuwen PL, Schalkwijk J. Coal tar induces AHR-dependent skin barrier repair in atopic dermatitis. *J Clin Invest*. 2013;123(2):917–927. doi:10.1172/jci65642.
24. Furue M. Regulation of flaggrin, loricrin, and involucrin by IL-4, IL-13, IL-17A, IL-22, AHR, and NRF2: pathogenic implications in atopic dermatitis. *Int J Mol Sci*. 2020;21(15):5382. doi:10.3390/ijms21155382.
25. Harima-Mizusawa N, Kamachi K, Kano M, Nozaki D, Uetake T, Yokomizo Y, Nagino T, Tanaka A, Miyazaki K, Nakamura S. Beneficial effects of citrus juice fermented with *Lactobacillus plantarum* YIT 0132 on atopic dermatitis: results of daily intake by adult patients in two open trials. *Biosci Microbiota Food Health*. 2016;35(1):29–39. doi:10.12938/bmfh.2015-010.
26. Yang J, McDowell A, Seo H, Kim S, Min TK, Jee YK, Choi Y, Park HS, Pyun BY, Kim YK. Diagnostic models for atopic dermatitis based on serum microbial extracellular vesicle metagenomic analysis: a pilot study. *Allergy Asthma Immunol Res*. 2020;12(5):792–805. doi:10.4168/aaair.2020.12.5.792.
27. Björkstén B, Naaber P, Sepp E, Mikelsaar M. The intestinal microflora in allergic Estonian and Swedish 2-year-old children. *Clin Exp Allergy*. 1999;29(3):342–346. doi:10.1046/j.1365-2222.1999.00560.x.
28. Enomoto T, Sowa M, Nishimori K, Shimazu S, Yoshida A, Yamada K, Furukawa F, Nakagawa T, Yanagisawa N, Iwabuchi N, et al. Effects of bifidobacterial supplementation to pregnant women and infants in the prevention of allergy development in infants and on fecal microbiota. *Allergol Int*. 2014;63(4):575–585. doi:10.2332/allergolint.13-OA-0683.
29. Kim IS, Lee SH, Kwon YM, Adhikari B, Kim JA, Yu DY, Kim GI, Lim JM, Kim SH, Lee SS, et al. Oral Administration of  $\beta$ -glucan and *Lactobacillus plantarum* alleviates atopic dermatitis-like symptoms. *J Microbiol Biotechnol*. 2019;29(11):1693–1706. doi:10.4014/jmb.1907.07011.
30. Akiyama T, Iodi Carstens M, Carstens E. Transmitters and pathways mediating inhibition of spinal itch-signaling neurons by scratching and other counterstimuli. *PLoS One*. 2011;6:e22665. doi:10.1371/journal.pone.0022665.

31. Park YM, Lee SY, Kang MJ, Kim BS, Lee MJ, Jung SS, Yoon JS, Cho HJ, Lee E, Yang SI, et al. Imbalance of gut *Streptococcus*, *Clostridium*, and *Akkermansia* determines the natural course of atopic dermatitis in infant. *Allergy Asthma Immunol Res.* 2020;12:322–337. doi:10.4168/aaair.2020.12.2.322.
32. Qian Y, Yang X, Xu S, Wu C, Song Y, Qin N, Chen SD, Xiao Q. Alteration of the fecal microbiota in Chinese patients with Parkinson's disease. *Brain Behav Immun.* 2018;70:194–202. doi:10.1016/j.bbi.2018.02.016.
33. Santos-Marcos JA, Haro C, Vega-Rojas A, Alcalá-Díaz JF, Molina-Abril H, Leon-Acuña A, Lopez-Moreno J, Landa BB, Tena-Sempere M, Perez-Martinez P, et al. Sex Differences in the gut microbiota as potential determinants of gender predisposition to disease. *Mol Nutr Food Res.* 2019;63(7):e1800870. doi:10.1002/mnfr.201800870.
34. Moon C, Baldrige MT, Wallace MA, Burnham CA, Virgin HW, Stappenbeck TS. Vertically transmitted faecal IgA levels determine extra-chromosomal phenotypic variation. *Nature.* 2015;521(7550):90–93. doi:10.1038/nature14139.
35. Kaakoush NO. *Sutterella* species, iga-degrading bacteria in ulcerative colitis. *Trends Microbiol.* 2020;28(7):519–522. doi:10.1016/j.tim.2020.02.018.
36. Williams BL, Hornig M, Parekh T, Lipkin WI. Application of novel PCR-based methods for detection, quantitation, and phylogenetic characterization of *Sutterella* species in intestinal biopsy samples from children with autism and gastrointestinal disturbances. *mBio.* 2012;3. doi:10.1128/mBio.00261-11.
37. Wang L, Christophersen CT, Sorich MJ, Gerber JP, Angley MT, Conlon MA. Increased abundance of *Sutterella* spp. and *Ruminococcus torques* in feces of children with autism spectrum disorder. *Mol Autism.* 2013;4(1):42. doi:10.1186/2040-2392-4-42.
38. Eetemadi A, Tagkopoulos I. Methane and fatty acid metabolism pathways are predictive of Low-FODMAP diet efficacy for patients with irritable bowel syndrome. *Clin Nutr.* 2021;40(6):4414–4421. doi:10.1016/j.clnu.2020.12.041.
39. Ta LDH, Chan JCY, Yap GC, Purbojati RW, Drautz-Moses DI, Koh YM, Tay CJX, Huang CH, Kioh DYQ, Woon JY, et al. A compromised developmental trajectory of the infant gut microbiome and metabolome in atopic eczema. *Gut Microbes.* 2020;12(1):1–22. doi:10.1080/19490976.2020.1801964.
40. Zhou W, Qi D, Swaisgood RR, Wang L, Jin Y, Wu Q, Wei F, Nie Y. Symbiotic bacteria mediate volatile chemical signal synthesis in a large solitary mammal species. *Isme j.* 2021;15(7):2070–2080. doi:10.1038/s41396-021-00905-1.
41. Franzosa EA, McIver LJ, Rahnavard G, Thompson LR, Schirmer M, Weingart G, Lipson KS, Knight R, Caporaso JG, Segata N, et al. Species-level functional profiling of metagenomes and metatranscriptomes. *Nat Methods.* 2018;15(11):962–968. doi:10.1038/s41592-018-0176-y.
42. Langille MG, Zaneveld J, Caporaso JG, McDonald D, Knights D, Reyes JA, Clemente JC, Burkpile DE, Vega Thurber RL, Knight R, et al. Predictive functional profiling of microbial communities using 16S rRNA marker gene sequences. *Nat Biotechnol.* 2013;31(9):814–821. doi:10.1038/nbt.2676.
43. Cervantes-Barragan L, Chai JN, Tianero MD, Di Luccia B, Ahern PP, Merriman J, Cortez VS, Caparon MG, Donia MS, Gilfillan S, et al. *Lactobacillus reuteri* induces gut intraepithelial CD4(+)CD8α(+) T cells. *Science.* 2017;357:806–810. doi:10.1126/science.aah5825.